iScience

Article

Vitamin D3 induces mesenchymal-to-endothelial transition and promotes a proangiogenic niche through IGF-1 signaling

Lei Chen,
Anweshan
Samanta, Lin
Zhao, ..., Jeryl
Hauptman, Magdy
Girgis,
Buddhadeb Dawn

buddha.dawn@unlv.edu

HIGHLIGHTS

Vitamin D3 (VitD3)
treatment induces IGF-1
in mesenchymal stem cells
(MSCs)

VitD3 promotes
mesenchymal-to-
endothelial transition in
MSCs via IGF-1 signaling

Continued IGF-1
secretion by VitD3-
treated MSCs creates a
proangiogenic niche

VitD3 may enhance MSC-
induced angiogenesis
through dual mechanisms

Article

Vitamin D3 induces mesenchymal-to-endothelial transition and promotes a proangiogenic niche through IGF-1 signaling

Lei Chen,[1] Anweshan Samanta,[2] Lin Zhao,[3] Nathaniel R. Dudley,[1] Tanner Buehler,[1] Robert J. Vincent,[1] Jeryl Hauptman,[3] Magdy Girgis,[3] and Buddhadeb Dawn[3,4,*]

SUMMARY

Although vitamin D3 (VitD3) prevents angiogenesis in cancer, VitD3 deficiency is associated with greater incidence of cardiovascular events in patients. We examined the influence of VitD3 on the angiogenic potential of mesenchymal stem cells (MSCs). VitD3 treatment increased the expression of proangiogenic molecules in MSCs, which exhibited an endothelial cell-like phenotype and promoted vascularization *in vitro* and *in vivo*. VitD3 activated the IGF-1 promoter and boosted IGF-1 receptor (IGF-1R) signaling, which was essential for the mesenchymal-to-endothelial transition (MEndoT) of MSCs. VitD3-treated MSCs created a proangiogenic microenvironment for co-cultured arterial endothelial cells, as well as aortic rings. The induction of MEndoT and angiogenesis promotion by VitD3-stimulated MSCs was attenuated by IGF-1R inhibitor picropodophyllin. We conclude that VitD3 promotes MEndoT in MSCs, and VitD3-treated MSCs augment vascularization by producing a proangiogenic niche through continued IGF-1 secretion. These results suggest a potential therapeutic role of VitD3 toward enhancing MSC-induced angiogenesis.

INTRODUCTION

Bone marrow mesenchymal stem cells (MSCs) have been shown to promote angiogenesis after an ischemic injury (Nagaya et al., 2004). Under specific culture conditions, a small fraction of MSCs express endothelial characteristics (Prockop, 1997). MSCs also participate in angiogenesis through paracrine factors, including vascular endothelial growth factors (VEGFs) and basic fibroblast growth factor (Kinnaird et al., 2004b). However, the results of clinical trials for therapeutic tissue repair with MSCs have produced suboptimal results.

Although vitamin D3 (VitD3) deficiency has been linked to manifold adverse health consequences (Holick, 2006), the underlying pathophysiology and molecular mechanisms remain largely unclear. The effects of VitD3 on angiogenesis remain particularly perplexing. VitD3 has also been shown to suppress endothelial cell sprouting and proliferation *in vitro* and reduce vascularity of tumors *in vivo* (Mantell et al., 2000). However, a role of VitD3 in the promotion of vascular regeneration through the SDF-1/CXCR4 axis and recruitment of angiogenic myeloid cells has been reported (Wong et al., 2014). The ability of VitD3 to enhance proliferation and migration of endothelial cells has also been documented (Molinari et al., 2013). In addition, epidemiological data from VitD3-deficient patients show an increased incidence of cardiovascular events (Wang et al., 2008), suggesting its possible proangiogenic influence.

Given the therapeutic potential of MSCs in cardiac repair (Golpanian et al., 2016), we sought to determine whether VitD3 treatment could induce a proangiogenic phenotype in MSCs and promote vascularization. We further investigated the impact of VitD3 treatment on MSC niche. Although a positive association between serum 25(OH)D levels and IGF-1 concentration in humans has been reported (Hypponen et al., 2008), the potential molecular basis remains unknown. Since IGF-1 is known to promote angiogenesis (van Beijnum et al., 2017) and has been reported to increase levels of VEGF and its receptors in certain cells (Menu et al., 2004; Rabinovsky and Draghia-Akli, 2004), we examined whether VitD3 treatment would induce mesenchymal-to-endothelial transition (MEndoT) through IGF-1 upregulation. Our results indicate that VitD3 induces MEndoT in MSCs and augment angiogenesis in a dose-dependent manner. Perhaps

[1]Department of Cardiovascular Medicine, University of Kansas Medical Center, Kansas City, KS, USA

[2]Department of Internal Medicine, University of Missouri-Kansas City, Kansas City, MO, USA

[3]Department of Internal Medicine, University of Nevada, Las Vegas School of Medicine, 1701 W. Charleston Boulevard, Suite 230, Las Vegas, NV 89102, USA

[4]Lead contact

*Correspondence:
buddha.dawn@unlv.edu

https://doi.org/10.1016/j.isci.2021.102272
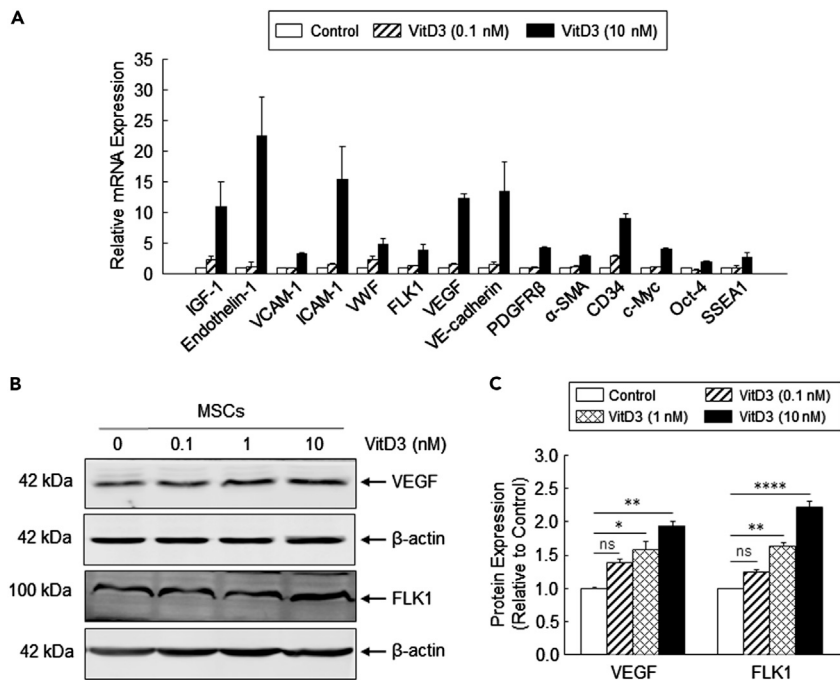
Figure 1. VitD3 induces proangiogenic molecules in MSCs

(A) qPCR data show increased mRNA levels of proangiogenic as well as pluripotency-related genes in MSCs following exposure to VitD3. Data represent mean $\pm$ standard error of the mean (SEM), n = 3.

(B) Representative Western immunoblots show VEGF, FLK1, and β-actin (loading control) protein levels in MSCs following VitD3 stimulation.

(C) Densitometric quantitation of VEGF and FLK1 protein levels.

Data represent mean $\pm$ SEM. One-way analysis of variance (ANOVA) with Bonferroni *post hoc* test, ns = not significant, *p < 0.05, **p < 0.01, ****p < 0.0001, n = 3.

more importantly, our findings also show that VitD3-treated MSCs are able to create a proangiogenic niche through increased IGF-1 secretion.

RESULTS

VitD3 induces proangiogenic genes and proteins in MSCs

The role of VitD3 in angiogenesis remains poorly understood. To examine the angiogenic potential of VitD3, we first examined whether exposure to VitD3 would increase the expression of molecules known to promote angiogenesis. MSCs were harvested from murine bone marrow by adhesion and expanded in culture. To analyze the expression profile of these genes, total RNA was extracted from MSCs after 48 h of treatment with VitD3 (0.1 nM and 10 nM) or dimethyl sulfoxide (DMSO, control). Quantitative polymerase chain reaction (qPCR) data in Figure 1A show that VitD3 treatment upregulated the expression of proangiogenic genes, including VEGF, FLK1, endothelin-1, VCAM-1, ICAM-1, VWF, and VE-cadherin in a dose-dependent fashion. The levels of 2 key proangiogenic molecules, VEGF and its receptor FLK1, increased 12.4- and 3.9-fold, respectively, with 10 nM of VitD3 (Figure 1A). Increased VEGF and FLK1 levels by Western blot analysis confirmed the above mRNA findings at the protein level (Figures 1B and 1C). Interestingly, the expression of genes associated with cellular pluripotency such as Oct-4 and SSEA1 was also upregulated by VitD3 treatment (Figure 1A).

VitD3 induces mesenchymal-to-endothelial transition in MSCs

Since the ability of VitD3 to induce endothelial transition in MSCs remains unknown, we examined whether VitD3 could induce this phenotypic shift in MSCs. Treatment of MSCs with VitD3 for 48 h increased VE-cadherin and CD34 protein levels in a dose-dependent manner (Figures 2A and 2B). These results were further validated by staining of MSCs with fluorophore-conjugated anti-VE-cadherin and anti-CD34 antibodies. As shown in Figure 2C, compared with control MSCs, VitD3-treated MSCs exhibited increased fluorescent
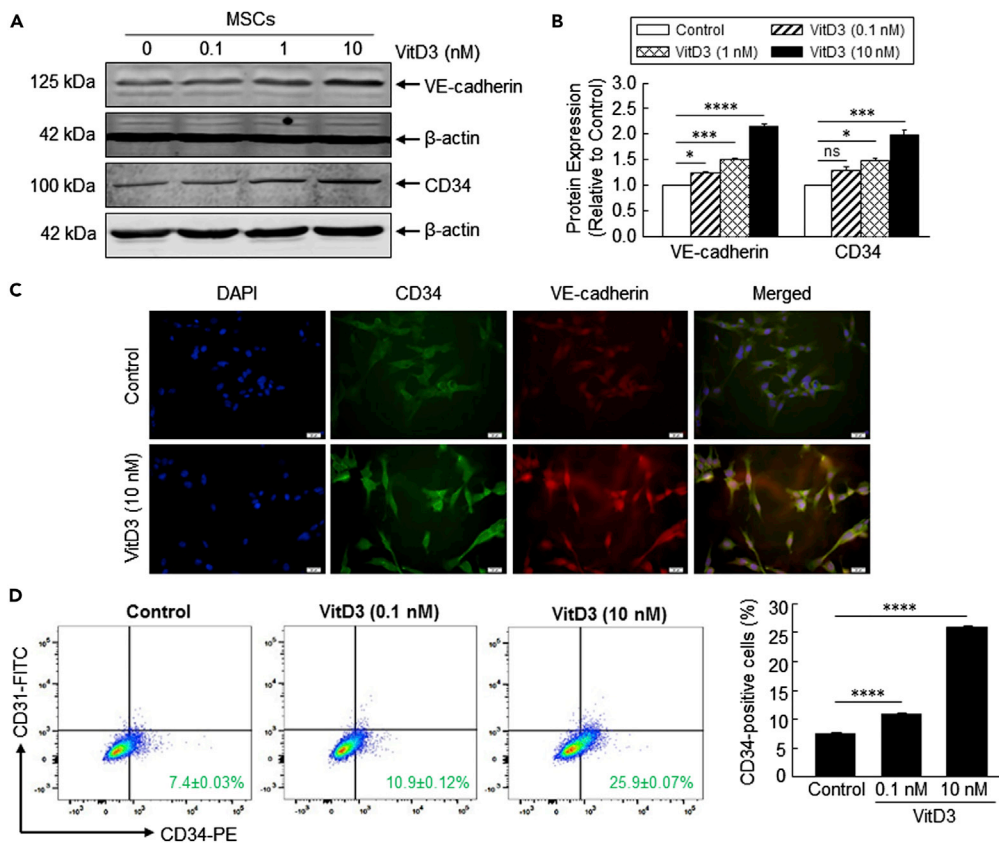
Figure 2. VitD3 induces MEndoT in MSCs

(A) Representative Western immunoblots show VE-cadherin, CD34, and β-actin (loading control) expression in MSCs following VitD3 stimulation.

(B) Densitometric quantitation of VE-cadherin and CD34 protein levels. Data represent mean ± standard error of the mean (SEM). One-way analysis of variance (ANOVA) with Bonferroni *post hoc* test, ns = not significant, *p < 0.05, ***p < 0.001, ****p < 0.0001, n = 3.

(C) Increased expression of CD34 (FITC, green) and VE-cadherin (TRITC, red) in MSCs following VitD3 treatment. Nuclei are identified in blue (DAPI). Scale bar, 20 μm.

(D) Flow cytometric analysis shows a dose-dependent increase in CD34 expression and minimal expression of CD31 in VitD3-stimulated MSCs. The right part shows the quantitative data. Data represent mean ± SEM. One-way ANOVA with Bonferroni *post hoc* test, ****p < 0.0001, n = 3.

signals indicating greater expression of VE-cadherin and CD34. As VE-cadherin is essential for cohesion and organization of the intercellular junctions of endothelial cells, it is a reliable indicator of an endothelial phenotype (Breier et al., 1996). These observations therefore suggest that a significant fraction of VitD3-treated MSCs acquire an endothelial-like cellular phenotype.

To quantify the extent of MEndoT, control and VitD3-treated MSCs were stained with fluorescent conjugated antibodies against CD34 and CD31, two known markers of endothelial lineage (Middleton et al., 2005). Flow cytometric analysis identified a dose-dependent increase in CD34+ MSCs by 1.5- and 3.5-folds in 0.1 nM and 10 nM VitD3-treated MSC groups, respectively, compared with control MSCs (Figure 2D). Interestingly, CD31 expression did not increase significantly following VitD3 treatment, indicating early commitment to endothelial lineage.

VitD3-treated MSCs induce angiogenesis *in vitro* and *in vivo*

To determine the significance of the above molecular changes, we examined whether MEndoT in VitD3-treated MSCs would translate into angiogenesis. MSCs were treated with VitD3 for 48 h, and angiogenesis assays were performed *in vitro* on Matrigel. Compared with controls, VitD3 treatment resulted in greater
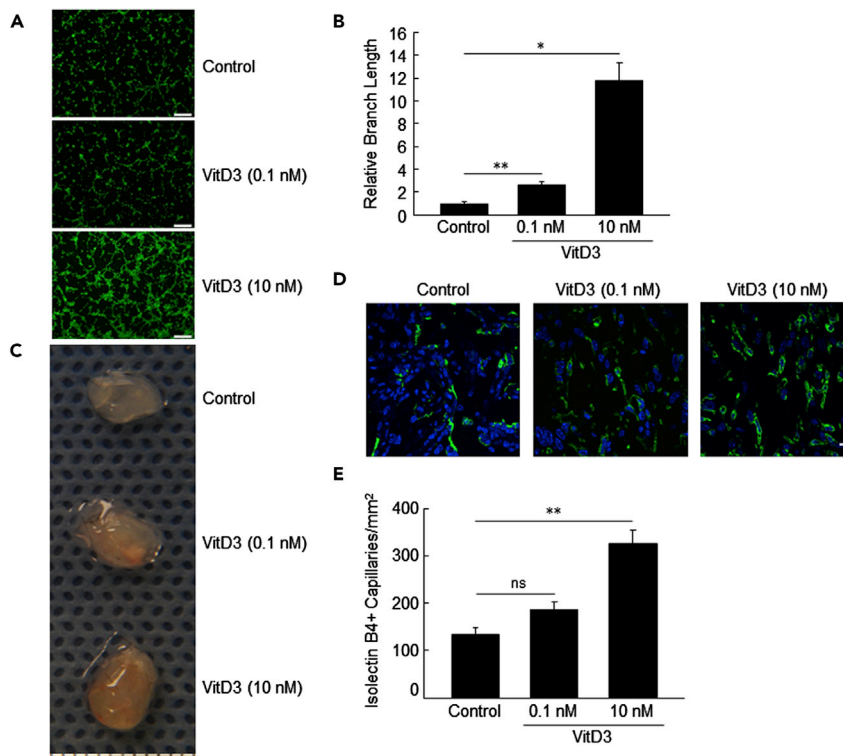
Figure 3. VitD3-treated MSCs promote angiogenesis *in vitro* and *in vivo*

(A) MSCs treated with either vehicle (control) or VitD3 produced a tube-like network in a Matrigel assay. Scale bar, 1 mm.

(B) Quantitative assessment of relative branch length. Data represent mean $\pm$ standard error of the mean (SEM), Welch's analysis of variance (ANOVA) with Dunnett's T3 *post hoc* test, *p < 0.05, **p < 0.01, n = 4.

(C) Explanted Matrigel plugs with vehicle- (control) or VitD3-treated MSCs show evidence of perfusion with blood. n = 6 per group.

(D) Isolectin B4 positivity (green) identifies capillary endothelium within Matrigel plugs at 3 weeks after implantation. Scale bar, 10 μm.

(E) Quantitative estimates of capillary densities in Matrigel plugs. Data represent mean $\pm$ SEM. One-way ANOVA with Bonferroni *post hoc* test, ns = not significant, **p < 0.01, n = 4 per group.

tube formation by MSCs (Figure 3A), which quantitatively resulted in 2.68- and 11.76-fold greater branch lengths in 0.1 nM and 10 nM VitD3-treated MSCs groups (Figure 3B), respectively.

Next, we performed a xenograft assay to examine whether MSCs were capable of promoting angiogenesis *in vivo*. Control Matrigel plugs or those mixed with VitD3-treated MSCs were transplanted subcutaneously in 8-week-old C57BL/6 male mice. Three weeks later, explanted Matrigel plugs carrying VitD3-treated MSCs macroscopically displayed a pink color indicating perfusion with blood *in vivo* as compared with a pale color observed in control MSC plugs (Figure 3C). The 10 nM VitD3-treated group showed a significantly darker change in coloration. This indicated the presence of larger amount of blood, which suggested a higher density of functional capillaries, an early stage marker of neovascularization produced by endothelial cells (Akhtar et al., 2002). Sections from Matrigel plugs were stained with isolectin B4 (Figure 3D) and capillary densities quantified using microscopy. The capillary densities were 1.41- and 2.46-folds greater in the 0.1 nM and 10 nM VitD3-treated MSC groups, respectively (Figure 3E). Together, these data indicate that MSCs treated with VitD3 are able to induce greater angiogenesis both *in vitro* and *in vivo*.

VitD3 induces and activates the IGF-1 proangiogenic signaling pathway

To elucidate the mechanistic basis of the above observations, we investigated the molecular events that lead to MEndoT of VitD3-treated MSCs. Earlier, we observed that the expression of IGF-1 in MSCs was significantly enhanced following VitD3 treatment (Figure 1A). To further validate this finding, protein expression of IGF-1 was assessed by Western blot analysis following 48 h of VitD3 treatment. We found
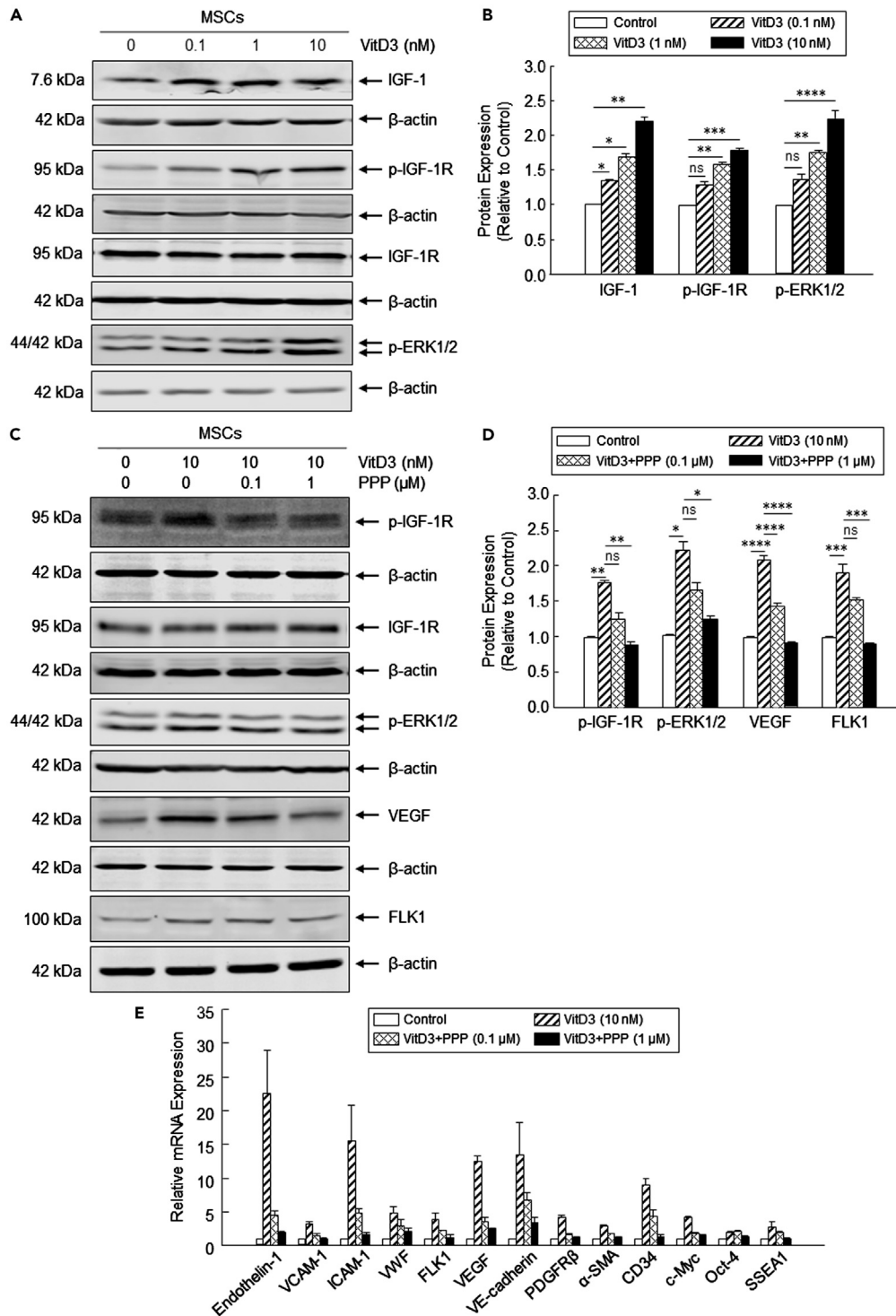
Figure 4. VitD3 enhances proangiogenic IGF-1 signaling in MSCs

(A and B) Representative Western immunoblots (A) and quantitative densitometric data (B) show increased protein expression of key components of IGF-1 signaling in VitD3-treated MSCs in a dose-dependent manner. Data represent mean ± standard error of the mean (SEM). Welch's analysis of variance (ANOVA) with Dunnett's T3 *post hoc* test (IGF-1 and p-IGF-1R) and one-way ANOVA with Bonferroni *post hoc* test (p-ERK1/2), ns = not significant, *p < 0.05, **p < 0.01, ***p < 0.001, ****p < 0.0001, n = 3.

Figure 4. *Continued*

(C and D) Representative Western immunoblots (C) and quantitative densitometric data (D) show reversal of VitD3-induced expression of proangiogenic molecules following co-treatment with PPP, an IGF-1R antagonist, in a dose-dependent manner. Data represent mean $\pm$ SEM. Welch's ANOVA with Dunnett's T3 *post hoc* test (p-IGF-1R and p-ERK1/2) and one-way ANOVA with Bonferroni *post hoc* test (VEGF and FLK1), ns = not significant, *p < 0.05, **p < 0.01, ***p < 0.001, ****p < 0.0001, n = 3.

(E) qPCR data show reversal of VitD3-induced increased expression of proangiogenic genes following co-treatment with PPP, an IGF-1R antagonist. Data represent mean $\pm$ SEM, n = 3.

significant upregulation of IGF-1 by VitD3 in a dose-dependent manner (Figures 4A and 4B). In light of these results, we examined the activation of IGF-1 receptor (IGF-1R) via phosphorylation. The phospho-IGF-1R levels increased by 1.28-, 1.60-, and 1.79-folds in 0.1 nM, 1 nM, and 10 nM VitD3-treated MSC groups, respectively. In addition, we found concomitant increases in the activation of a key downstream factor for angiogenesis, phospho-ERK1/2 (Dunn et al., 2001) (Figures 4A and 4B). To further interrogate the role of IGF-1 signaling in VitD3-treated MSCs, we analyzed IGF-1R signaling using a specific inhibitor, picropodophyllin (PPP). The VitD3-induced increase in phospho-IGF-1R, phospho-ERK1/2, VEGF, and FLK1 was reduced by co-treatment with PPP, and this suppression was also dose dependent (Figures 4C and 4D).

Although IGF-1 signaling has been shown to promote angiogenesis, its role in MSC-induced angiogenesis remains unknown. To address this, qPCR was performed to examine the relative levels of mRNA transcripts encoding proangiogenic factors following treatment with VitD3 with or without PPP. VitD3 treatment resulted in marked increase in mRNA expression of several proangiogenic and pluripotency-related molecules. PPP co-treatment reversed these changes with suppression of VitD3-induced augmentation of mRNA expression of endothelin-1, VCAM-1, ICAM-1, VE-cadherin, VWF, PDGFRβ, α-SMA, CD34, FLK1, and VEGF (Figure 4E), indicating that VitD3-induced activation of IGF-1R signaling is responsible for the induction of a proangiogenic phenotype in MSCs.

To further substantiate these findings at the mRNA level, we performed Western blot analysis using protein samples from cells subjected to analogous treatments. The results confirmed similar effects of PPP co-treatment on protein levels of VE-cadherin and CD34 (Figure 5A). Finally, MSCs treated with VitD3 with/out PPP for 48 h were stained with anti-VE-cadherin and anti-CD34 antibodies followed by fluorescent imaging. Consistently, the VitD3-induced increase in fluoresence signals of VE-cadherin and CD34 was markedly reduced in MSCs co-treated with PPP (Figure 5B).

VEGF and FLK1 (Figures 4C and 4D) are two of the most important proangiogenic signaling molecules. Thus, suppression of VEGF and FLK1 expression by PPP indicated a negative impact of PPP on angiogenesis by MSCs. To examine this, VitD3-treated MSCs with or without PPP co-treatment were subjected to an *in vitro* angiogenesis assay on Matrigel. As shown in Figure 5C, the branch formation competence of MSCs was greatly reduced by PPP. Compared with untreated MSCs (control), branch length increased by 11.76-fold in the VitD3-treated MSC group, which was reduced to a mere 3.45-fold increase with PPP co-treatment (Figure 5D). The suppression of both angiogenesis-related gene expression and branch formation by IGF-1R inhibitor PPP indicates that IGF-1, through the expression of VEGF-FLK1, is a major factor contributing to the angiogenesis-promoting effects of VitD3 in MSCs.

IGF-1 identified as the target gene for VitD3

The functions of VitD3 are predominantly activated through binding to its specific receptor, the vitamin D receptor (VDR) (Brumbaugh and Haussler, 1973). To determine whether the VitD3-VDR complex is a transcriptional activator of IGF-1, chromatin immunoprecipitation (ChIP) assay was performed for IGF-1 in response to VitD3 treatment of MSCs. The results of the ChIP assay indicated that VDR directly binds to the promoter region of IGF-1 and that this binding was more robust in the presence of increasing doses of VitD3 (Figure 6A). Compared with untreated MSC controls, the VDR binding activities were 7.28- and 43.76-folds greater in MSCs treated with 0.1 nM and 10 nM of VitD3, respectively (Figure 6B).

Furthermore, the analysis of murine IGF-1 genomic sequence identified two potential VDR response elements in the promoter region of IGF-1. Next, to evaluate whether these response elements within the IGF-1 promoter confer VitD3 and VDR-dependent transcriptional activation, luciferase assay was performed. A DNA fragment of the IGF-1 promoter was subcloned into the firefly luciferase reporter vector,
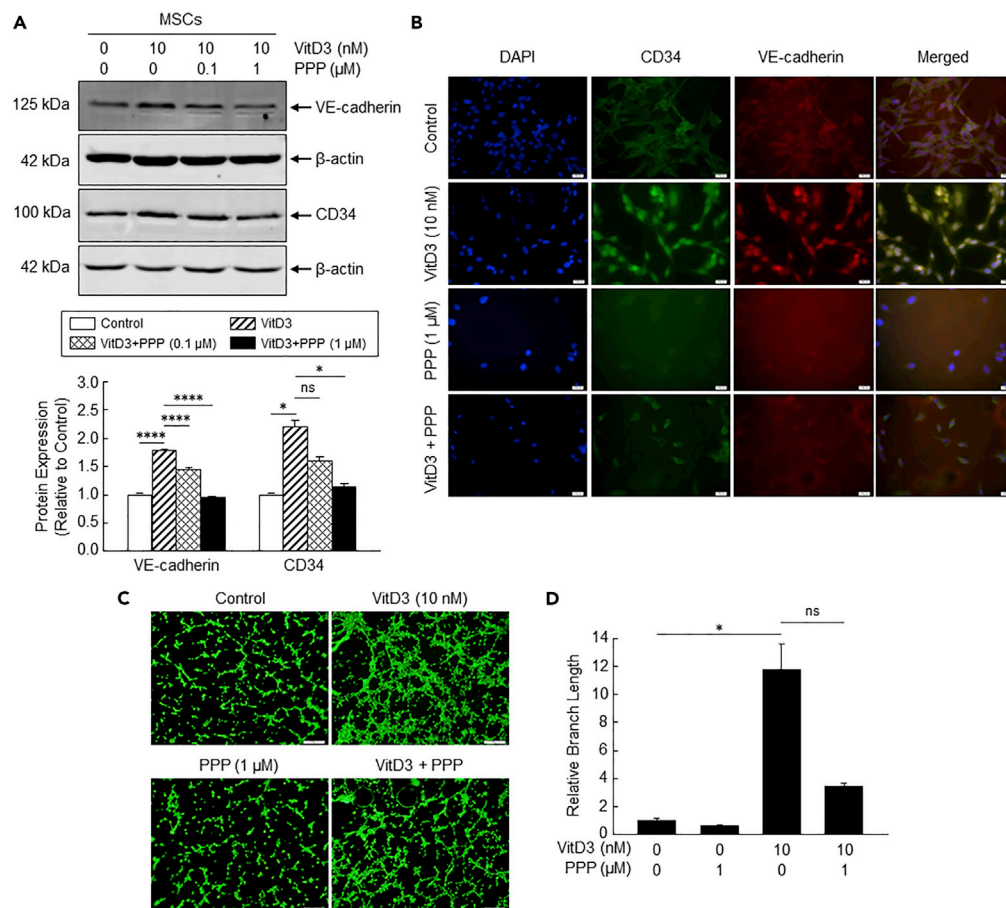
Figure 5. IGF-1R antagonist inhibits both MEndoT and the proangiogenic phenotype of VitD3-treated MSCs

(A) Representative Western immunoblots (upper panel) and quantitative densitometric data (lower panel) show dose-dependent reversal of VitD3-induced increase in VE-cadherin and CD34 levels in VitD3-treated MSCs with PPP co-treatment. Data represent mean ± standard error of the mean (SEM). One-way analysis of variance (ANOVA) with Bonferroni *post hoc* test (VE-cadherin) and Welch's ANOVA with Dunnett's T3 *post hoc* test (CD34), ns = not significant, *p < 0.05, ****p < 0.0001, n = 3.

(B) The inhibition of VitD3-induced angiogenic phenotype in MSCs by IGF-1R antagonist PPP was further confirmed with fluorescent detection of VE-cadherin (red) and CD34 (green) in MSCs treated with VitD3 with and without PPP. Scale bar, 20 μm.

(C and D) Representative images (C) and quantitative assessment of branch length (D) show robust augmentation of capillary-like tube formation by MSCs on Matrigel following VitD3 treatment and inhibition of the same by co-treatment with IGF-1R antagonist PPP. Scale bar, 100 μm.

Data represent mean ± SEM. Welch's ANOVA with Dunnett's T3 *post hoc* test, ns = not significant, *p < 0.05, n = 4.

pGL3-Basic (renamed IGF-1-WT). In addition, the VDR binding elements within the IGF-1 promoter region were mutated and subcloned into the pGL3-Basic vector and renamed IGF-1-mut1 and IGF-1-mut2 (Figure 6C). As shown in Figure 6D, the induction of the luciferase signal was enhanced by 1.43- and 4.32-folds in MSCs treated with 0.1 nM and 10 nM of VitD3, respectively, compared with controls, suggesting that VitD3, through its activation of the VDR, can activate IGF-1 expression. The respective reporter signals of the IGF-1-mutants induced by VitD3 were considerably less when compared with the wild-type IGF-1 promoter vector (IGF-1-WT) during stimulation with the same concentrations of VitD3 (Figure 6D), confirming the role of VDR binding to IGF-1 promoter in response to VitD3 stimulation.

VitD3-treated MSCs promote a proangiogenic niche

MSCs have the ability to generate a specific microenvironment through the secretion of various factors (Kinnaird et al., 2004a, 2004b). Our results show the ability of VitD3 treatment to induce IGF-1 expression in
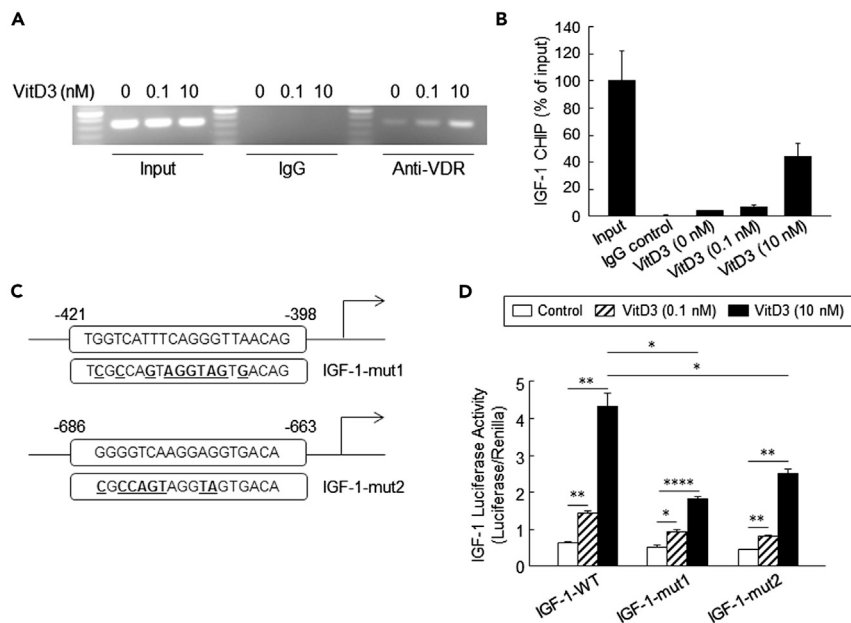
Figure 6. VitD3/VDR directly binds to the IGF-1 promoter and increases activity

(A and B) The binding of VDR following VitD3 stimulation in MSCs was analyzed by ChIP assay (A) and the relative densities of DNA bands were quantified (B). Data represent mean ± standard error of the mean (SEM). n = 4.

(C) The potential VDR response elements within the promoter region of IGF-1 (top) and the corresponding mutant VDR response elements (bottom, with mutated nucleotides underlined).

(D) Luciferase reporter constructs containing either wild-type or mutant promoter sequences were transfected into MSCs for VitD3 stimulation, and the relative levels of luciferase were analyzed following quantification with the internal control. Data represent mean ± SEM. One-way or Welch's analysis of variance (ANOVA) with Bonferroni or Dunnett's T3 *post hoc* tests, respectively, *p < 0.05, **p < 0.01, ****p < 0.0001, n = 3.

MSCs (Figures 1A and 4A). As a secreted protein, IGF-1 has the potential to produce a niche within the surrounding cells by binding to its cognate receptor. To evaluate this niche-forming ability of IGF-1, MSCs were subjected to either 0.1 nM or 10 nM of VitD3 for 3 days and then cultured in fresh media (without VitD3) for an additional 5 days. The IGF-1 concentrations in the culture media were quantified by enzyme-linked immunosorbent assay (ELISA) on days 1, 2, 3, 4, 5, 6, and 8. The IGF-1 concentration in culture media increased significantly by day 3 with VitD3 stimulation. Compared with the 0.07 ng/mL of IGF-1 in control MSC media, IGF-1 levels in 0.1 nM and 10 nM VitD3-treated MSC groups were 0.44 ng/mL and 0.50 ng/mL, respectively. After switching to VitD3-free culture media, the IGF-1 concentration decreased slightly on day 4 but then continued to rise subsequently despite the removal of VitD3 stimulation. The IGF-1 levels in media containing non-treated MSCs (control) were low (Figure 7A). The IGF-1 levels in media containing MSCs previously treated with 10 nM of VitD3 were greater compared with levels in 0.1 nM of VitD3-treated MSCs or control MSCs (Figure 7A).

To examine the paracrine functionality of this niche, MSCs were treated with 10 nM of VitD3 for 3 days and then changed to fresh medium before co-culture experiments with endothelial cells (Figure 7B). Primary mouse pulmonary artery endothelial cells (MAECs) were incubated with Cytodex-3 beads, transplanted into a fibrinogen pad, and maintained in culture. After 3 to 5 days of co-culture in VitD3-free EGM-2MV medium, MAEC beads were co-cultured with MSCs without contact (Figure 7B). Compared with vehicle control, co-culturing with untreated MSCs (MSC-control) did not enhance branching (Figures 7C and 7D). However, MAECs co-cultured with VitD3-treated MSCs exhibited significantly more branching compared with MAECs co-cultured with control MSCs. The mean branch length was approximately 2.24-folds greater and mean protrusions per bead was approximately 4-folds higher in the group co-cultured with VitD3-treated MSCs compared with respective parameters in the MSC-control group (Figure 7D). However, the increase in branch length and the number of protrusions from MAEC beads co-cultured with VitD3-treated MSCs were significantly suppressed by the addition of 1 μM of PPP in the co-culture medium (Figures 7C and 7D). To further substantiate the niche-enhancing attributes of VitD3-treated MSCs,
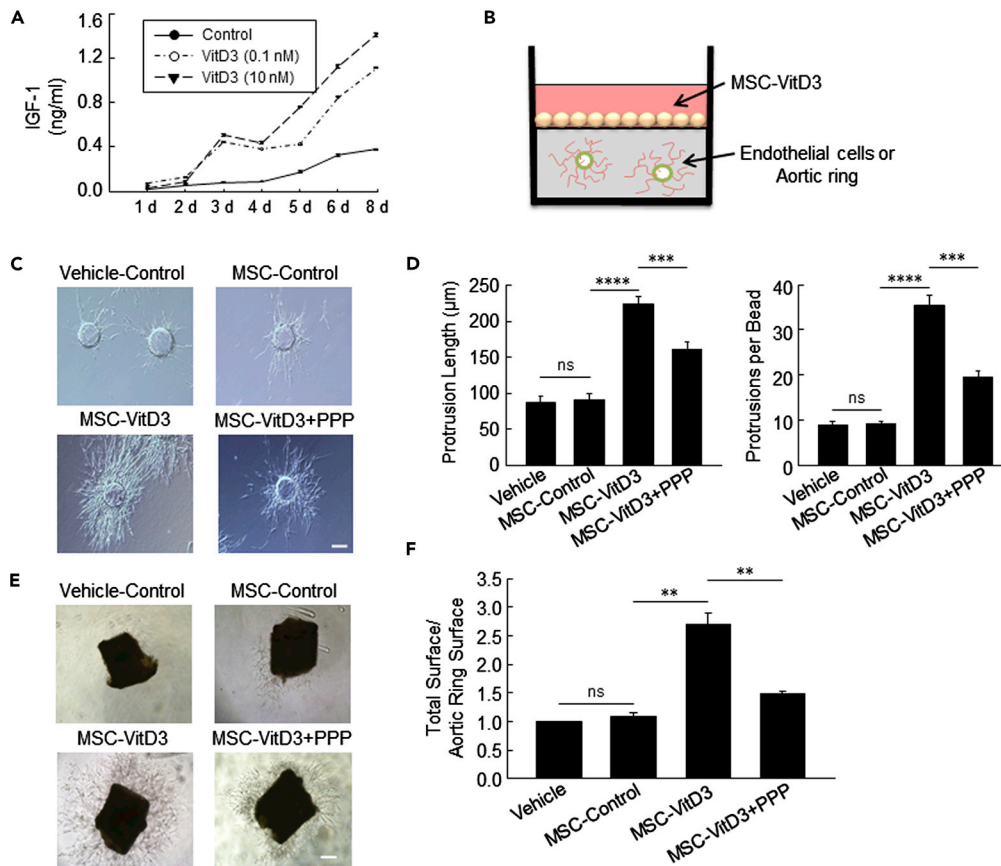
Figure 7. VitD3-treated MSCs produce an IGF-1 microenvironment for angiogenesis

(A) IGF-1 levels increase in the culture medium in a dose-dependent manner following exposure of MSCs to VitD3. IGF-1 levels continue to increase even after cessation of VitD3 stimulation. Data represent mean ± standard error of the mean (SEM). n = 3.

(B) Cartoon showing the experimental set up with VitD3-treated MSCs in contactless co-culture.

(C and D) Representative images (C) and quantitative data (D) show significant augmentation of bead branching with VitD3-treated MSCs and reversal of the same with VitD3 and PPP co-stimulated MSCs. Scale bar, 100 μm. Data represent mean ± SEM. One-way analysis of variance (ANOVA) with Bonferroni *post hoc* test (protrusion length) and Welch's ANOVA with Dunnett's T3 *post hoc* test (protrusions per bead), ns = not significant, ***p < 0.001, ****p < 0.0001, n = 8-10 per group.

(E and F) Representative images (E) and quantitative assessment of neovascularization surface area (F) from the aortic ring assay show enhanced sprouting induced by VitD3-treated MSCs. This effect was neutralized when MSCs were treated with PPP. Scale bar, 100 μm. Data represent mean ± SEM. Welch's ANOVA with Dunnett's T3 *post hoc* test, ns = not significant, **p < 0.01, n = 5 per group.

we also performed similar co-culture assays with murine aortic rings. Pieces of thoracic aorta harvested from 8-week-old C57BL/6 male mice were cut into 1-mm rings, embedded in Matrigel, and co-cultured with vehicle, control MSCs, or VitD3-treated MSCs as above. After 5 days, greater micro-vessel outgrowths surrounding the aortic rings were noted in co-cultures with VitD3-treated MSCs as compared with the MSC-control group (Figures 7E and 7F). This enhancement in outgrowths was suppressed by the addition of PPP to co-culture (Figures 7E and 7F). Together, these results identify IGF-1 as the primary factor secreted by VitD3-treated MSCs that produces a niche conducive for angiogenesis.

DISCUSSION

The role of VitD3 in angiogenesis remains controversial. Our findings establish a proangiogenic influence of VitD3 on MSCs, which have been used in clinical trials of cardiac repair with mixed results. The salient findings include the following: (i) treatment with VitD3 induces proangiogenic genes, increases the expression of endothelial markers, and promotes MEndoT in MSCs;(ii) VitD3-treated MSCs induce angiogenesis

both *in vitro* and *in vivo* in an IGF-1-dependent manner; (iii) VitD3/VDR complex binds to the IGF-1 promoter to induce IGF-1 expression; and (iv) VitD3 promotes the formation of a proangiogenic niche by MSCs through enhanced IGF-1 secretion. These results from both *in vitro* and *in vivo* studies underscore a beneficial role of VitD3 in vascular health through angiogenesis. This is particularly appealing because MSCs have therapeutic potential for diverse diseases, including cardiovascular ischemic diseases (Afzal et al., 2015; Golpanian et al., 2016). The current data bid well for successful clinical translation of VitD3-treated MSCs for vasculogenesis in patients with ischemic conditions.

Although sparse evidence suggests that VitD3 can influence cellular fate and inhibit epithelial to mesenchymal transition of cancer cells (Upadhyay et al., 2013), its role in endothelial transformation of mesenchymal cells remains unknown. The commitment to endothelial cell lineage is important because it increases the capacity for angiogenesis and capillary formation (Ribatti and Crivellato, 2012). The current results show upregulation of endothelial genes in VitD3-treated MSCs, which is corroborated by increased expression of both VE-cadherin and CD34, distinctive cell surface markers of endothelial lineage (Breier et al., 1996; Middleton et al., 2005). Together, these results establish the induction of MEndoT in VitD3-treated MSCs. The upregulation of other endothelial-related genes including VWF, ICAM-1, and VCAM-1 further establishes the endothelial nature of MSCs treated with VitD3.

The current results show an increased expression of IGF-1 in MSCs in response to VitD3 treatment. In addition, the increase in phospho-IGF-1R in VitD3-treated MSCs indicated the activation of IGF-1 signaling in these cells. In previous studies, IGF-1 has been shown to stimulate migration and tube-forming activities of endothelial cells, supporting a proangiogenic role (Nakao-Hayashi et al., 1992). The current data also show that the inhibition of IGF-1 signaling by PPP attenuated the induction of proangiogenic genes and blocked the acquisition of an endothelial phenotype by VitD3-treated MSCs, indicating a causal role of IGF-1 signaling toward VitD3-induced MEndoT. Concomitant exposure to PPP reduced the ability of VitD3-treated MSCs to form tubes on Matrigel, consistent with reduced capacity for angiogenesis. The mechanistic basis of IGF-1 induction by VitD3 was further confirmed by the ChIP assay that showed increased binding of the VitD3 response region on the IGF-1 promoter with increasing doses of VitD3. Collectively, these findings identify an important role of IGF-1 as the molecular link between VitD3 treatment and induction of MEndoT in MSCs.

Interestingly, IGF-1 produced in VitD3-treated MSCs exerted additional biological function beyond the induction of MEndoT. Our data show that IGF-1 continued to be secreted by VitD3-treated MSCs, even after VitD3 was removed from the culture medium. This prolonged secretion of IGF-1 by MSCs enhances an angiogenic niche conducive to the formation of new vasculature. Indeed, in our contactless co-culture system, VitD3-treated MSCs were able to induce angiogenesis in both MAECs and murine aortic rings. These observations suggest that following *in vivo* transplantation, VitD3-treated MSCs may induce angiogenesis through IGF-1-mediated niche formation in recipient tissues.

The precise role of VitD3 in endothelial cell biology and function may vary depending on the context (Jamali et al., 2018). Although an inhibitory influence of VitD3 on angiogenesis has been reported in the setting of malignancy (Mantell et al., 2000), epidemiological studies have identified an adverse association between VitD3 deficiency and incident cardiovascular events (Wang et al., 2008). In this context, the current findings identify two important mechanisms (Figure 8) through which VitD3 may augment vascularization. First, the generation of angiogenic cells from transplanted MSCs through VitD3-induced MEndoT may play a direct role toward increasing vascularity. Our data show an important role of VitD3-induced IGF-1 in this conversion of MSCs into cells that may directly effect angiogenesis. Second, the protracted secretion of IGF-1 by VitD3-treated MSCs may amplify the vasculogenic effects of donor MSCs by enabling the formation of proangiogenic niches at sites of MSC transplantation, with potential recruitment of host cells and additional vascularization. Collectively, these observations support an important role of VitD3 toward the promotion of angiogenesis, and may explain the increased cardiovascular events in patients with VitD3 deficiency. These findings also support the potential efficacy of VitD3-treated MSCs for therapeutic angiogenesis in ischemic tissues.

Limitations of the study

Although epidemiological evidence has identified an association between VitD3 deficiency and adverse cardiovascular events, it is difficult to reproduce the vascular effects of human VitD3 deficiency in isolation
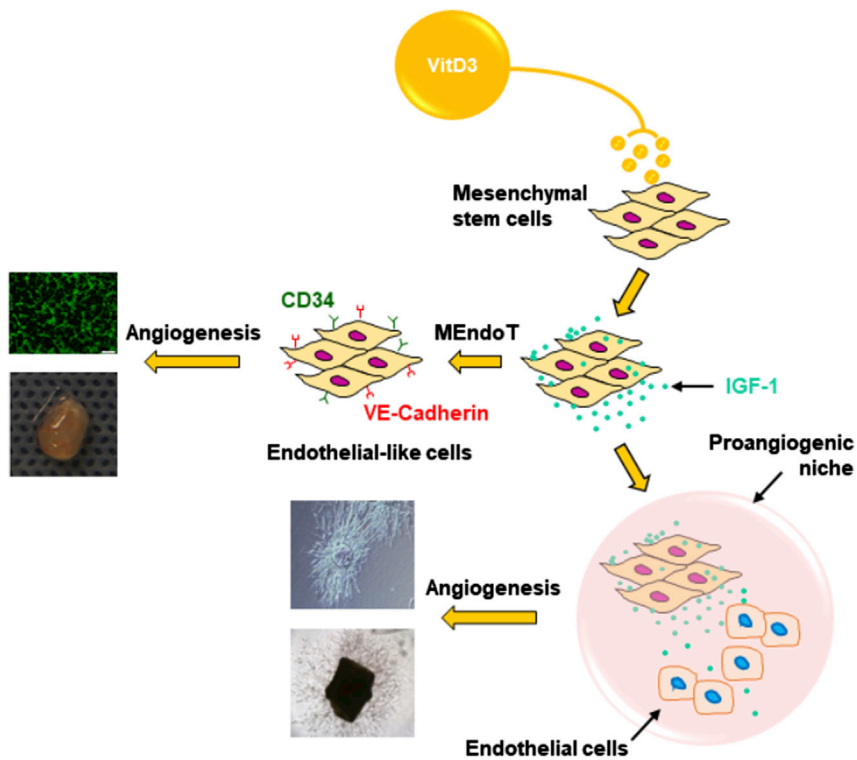
Figure 8. Schematic representation of dual mechanisms underlying VitD3-induced angiogenesis
VitD3 induces IGF-1 in MSCs, which promotes angiogenesis through MEndoT. In addition, VitD3-treated MSCs continue to secrete IGF-1, thereby creating a proangiogenic niche, which further amplifies the angiogenic effects of VitD3.

in a mouse model. Therefore, we focused on the elucidation of potential mechanisms through which VitD3 may exert vascular benefits. Although our current results identify how VitD3 signaling may influence angiogenesis, additional studies in a model of ischemia and VitD3-treated MSC transplantation *in vivo* will be necessary in the future.

Resource availability

Lead contact
Further information and request for resources and reagents should be directed to Prof. Buddhadeb Dawn (buddha.dawn@unlv.edu).

Materials availability
Any unique reagent or material will be available from the lead contact upon request.

Data and code availability
The published article includes all data generated or analyzed during this study. This study did not generate any unique code.

METHODS

All methods can be found in the accompanying transparent methods supplemental file.

SUPPLEMENTAL INFORMATION

Supplemental information can be found online at https://doi.org/10.1016/j.isci.2021.102272.

ACKNOWLEDGMENTS

AUTHOR CONTRIBUTIONS

DECLARATION OF INTERESTS

REFERENCES

Afzal, M.R., Samanta, A., Shah, Z.I., Jeevanantham, V., Abdel-Latif, A., Zuba-Surma, E.K., and Dawn, B. (2015). Adult bone marrow cell therapy for ischemic heart disease: evidence and insights from randomized controlled trials. Circ. Res. 117, 558–575.

Akhtar, N., Dickerson, E.B., and Auerbach, R. (2002). The sponge/Matrigel angiogenesis assay. Angiogenesis 5, 75–80.

Breier, G., Breviario, F., Caveda, L., Berthier, R., Schnurch, H., Gotsch, U., Vestweber, D., Risau, W., and Dejana, E. (1996). Molecular cloning and expression of murine vascular endothelial-cadherin in early stage development of cardiovascular system. Blood 87, 630–641.

Brumbaugh, P.F., and Haussler, M.R. (1973). Nuclear and cytoplasmic receptors for 1,25-dihydroxycholecalciferol in intestinal mucosa. Biochem. Biophys. Res. Commun. 51, 74–80.

Dunn, S.E., Torres, J.V., Oh, J.S., Cykert, D.M., and Barrett, J.C. (2001). Up-regulation of urokinase-type plasminogen activator by insulin-like growth factor-I depends upon phosphatidylinositol-3 kinase and mitogen-activated protein kinase kinase. Cancer Res. 61, 1367–1374.

Golpanian, S., Wolf, A., Hatzistergos, K.E., and Hare, J.M. (2016). Rebuilding the damaged heart: mesenchymal stem cells, cell-based therapy, and engineered heart tissue. Physiol. Rev. 96, 1127–1168.

Holick, M.F. (2006). High prevalence of vitamin D inadequacy and implications for health. Mayo Clin. Proc. 81, 353–373.

Hypponen, E., Boucher, B.J., Berry, D.J., and Power, C. (2008). 25-hydroxyvitamin D, IGF-1, and metabolic syndrome at 45 years of age: a cross-sectional study in the 1958 British Birth Cohort. Diabetes 57, 298–305.

Jamali, N., Sorenson, C.M., and Sheibani, N. (2018). Vitamin D and regulation of vascular cell function. Am. J. Physiol. Heart Circ. Physiol. 314, H753–H765.

Kinnaird, T., Stabile, E., Burnett, M.S., Lee, C.W., Barr, S., Fuchs, S., and Epstein, S.E. (2004a). Marrow-derived stromal cells express genes encoding a broad spectrum of arteriogenic cytokines and promote in vitro and in vivo arteriogenesis through paracrine mechanisms. Circ. Res. 94, 678–685.

Kinnaird, T., Stabile, E., Burnett, M.S., Shou, M., Lee, C.W., Barr, S., Fuchs, S., and Epstein, S.E. (2004b). Local delivery of marrow-derived stromal cells augments collateral perfusion through paracrine mechanisms. Circulation 109, 1543–1549.

Mantell, D.J., Owens, P.E., Bundred, N.J., Mawer, E.B., and Canfield, A.E. (2000). 1 alpha,25-dihydroxyvitamin D(3) inhibits angiogenesis in vitro and in vivo. Circ. Res. 87, 214–220.

Menu, E., Kooijman, R., Van Valckenborgh, E., Asosingh, K., Bakkus, M., Van Camp, B., and Vanderkerken, K. (2004). Specific roles for the PI3K and the MEK-ERK pathway in IGF-1-stimulated chemotaxis, VEGF secretion and proliferation of multiple myeloma cells: study in the 5T33MM model. Br. J. Cancer 90, 1076–1083.

Middleton, J., Americh, L., Gayon, R., Julien, D., Mansat, M., Mansat, P., Anract, P., Cantagrel, A., Cattan, P., Reimund, J.M., et al. (2005). A comparative study of endothelial cell markers expressed in chronically inflamed human tissues: MECA-79, Duffy antigen receptor for chemokines, von Willebrand factor, CD31, CD34, CD105 and CD146. J. Pathol. 206, 260–268.

Molinari, C., Rizzi, M., Squarzanti, D.F., Pittarella, P., Vacca, G., and Reno, F. (2013). 1alpha,25-Dihydroxycholecalciferol (Vitamin D3) induces NO-dependent endothelial cell proliferation and migration in a three-dimensional matrix. Cell Physiol. Biochem. 31, 815–822.

Nagaya, N., Fujii, T., Iwase, T., Ohgushi, H., Itoh, T., Uematsu, M., Yamagishi, M., Mori, H., Kangawa, K., and Kitamura, S. (2004). Intravenous administration of mesenchymal stem cells improves cardiac function in rats with acute myocardial infarction through angiogenesis and myogenesis. Am. J. Physiol. Heart Circ. Physiol. 287, H2670–H2676.

Nakao-Hayashi, J., Ito, H., Kanayasu, T., Morita, I., and Murota, S. (1992). Stimulatory effects of insulin and insulin-like growth factor I on migration and tube formation by vascular endothelial cells. Atherosclerosis 92, 141–149.

Prockop, D.J. (1997). Marrow stromal cells as stem cells for nonhematopoietic tissues. Science 276, 71–74.

Rabinovsky, E.D., and Draghia-Akli, R. (2004). Insulin-like growth factor I plasmid therapy promotes in vivo angiogenesis. Mol. Ther. 9, 46–55.

Ribatti, D., and Crivellato, E. (2012). Sprouting angiogenesis", a reappraisal. Dev. Biol. 372, 157–165.

Upadhyay, S.K., Verone, A., Shoemaker, S., Qin, M., Liu, S., Campbell, M., and Hershberger, P.A. (2013). 1,25-Dihydroxyvitamin D3 (1,25(OH)2D3) signaling capacity and the epithelial-mesenchymal transition in non-small cell lung cancer (NSCLC): implications for use of 1,25(OH)2D3 in NSCLC treatment. Cancers 5, 1504–1521.

van Beijnum, J.R., Pieters, W., Nowak-Sliwinska, P., and Griffioen, A.W. (2017). Insulin-like growth factor axis targeting in cancer and tumour angiogenesis - the missing link. Biol. Rev. Camb. Philos. Soc. 92, 1755–1768.

Wang, T.J., Pencina, M.J., Booth, S.L., Jacques, P.F., Ingelsson, E., Lanier, K., Benjamin, E.J., D'Agostino, R.B., Wolf, M., and Vasan, R.S. (2008). Vitamin D deficiency and risk of cardiovascular disease. Circulation 117, 503–511.

Wong, M.S., Leisegang, M.S., Kruse, C., Vogel, J., Schurmann, C., Dehne, N., Weigert, A., Herrmann, E., Brune, B., Shah, A.M., et al. (2014). Vitamin D promotes vascular regeneration. Circulation 130, 976–986.

Supplemental information

Vitamin D3 induces mesenchymal-to-endothelial

transition and promotes a proangiogenic niche

through IGF-1 signaling

Lei Chen, Anweshan Samanta, Lin Zhao, Nathaniel R. Dudley, Tanner Buehler, Robert J. Vincent, Jeryl Hauptman, Magdy Girgis, and Buddhadeb Dawn

TRANSPARENT METHODS

Animal Care and Use
The current study was approved by the Animal Care and Use Committee of the University of Kansas Medical Center, and performed in accordance with the Guide for the Care and Use of laboratory Animals (Department of Health and Human Service, Publication No. [NIH] 86-23).

Mesenchymal Stem Cell Isolation and Culture
Mesenchymal stem cells (MSCs) were collected from bone marrow as described previously with modifications (Labedz-Maslowska et al., 2015). In brief, the cavities of tibia and femur bones were collected from 8-week old male C57BL/6 mice by flushing with DMEM/F-12 media. The flushed cells were then purified with Ficoll balanced liquid (GE healthcare, 17-1440-02) and plated for 72 h, following which nonadherent cells were discarded, and adherent MSCs expanded in complete medium (DMEM/F-12 with 10% FBS).

Antibodies and Reagents
Antibodies against the following protein/epitopes were used in this study: CD34 (NOVUS; NB600-1071), VE-cadherin (NOVUS; AF1002), VEGF (Santa Cruz; sc-152), FLK1 (Santa Cruz; sc-57135), VDR (Cell Signaling; 12550), IGF-1 (Santa Cruz; sc-1422), IGF-1R (Cell Signaling; #9750), phospho-IGF-1R (Cell Signaling; #3021), phospho-ERK1/2 (Cell Signaling; #4370), ß-Actin (Santa Cruz; sc-1616) and PE-labeled CD34 (BD Biosciences, 551387), FITC-labeled CD31 (eBioscience, E00252-1631).

Reagents were obtained from the following sources: DMEM with high glucose were from Gibco (11330-032); EGM-2MV endothelial cell culture buckets were from Lonza (cc-3162); FITC-labeled Isolectin B4 were from Vector Laboratories Ltd; Fetal Bovine Serum (FBS) was from Gibco; qPCR amplification kits were purchased from Midsci; Matrigel matrix was from BD Biosciences. The luciferase reporter assay kit was from Promega. The IGF-1R specific inhibitor PPP, VitD3, Fibrinogen and the Cytobeads-3 were all from Sigma. The CellTrace™ Calcein Green, AM was from ThermoFisher Scientific (C34852). The IGF-1 mouse ELISA Kit was from Invitrogen (EMIGF1).

Capillary-like Tube Formation Assay
The capillary-like tube formation assay was performed as previously described (Khoo et al., 2011). Briefly, twenty-four well plates were coated with 100 μL/well of Matrigel matrix (BD Biosciences, 354267) and incubated at 37°C for 30 min. VitD3-treated MSCs and control MSCs were seeded at a density of 1×10^5 cells/well in the EGM-2MV media. Cells were incubated for 6 h at 37°C and stained with CellTrace™ Calcein Green, AM. Tube formation was examined every 2 h and phase-contrast images of MSC-derived cells on Matrigel were acquired with an Olympus IX71 inverted microscope. Tube length on four digital images from each group was measured using ImagePro Plus software, and the total length of branches on each image was calculated. These data were expressed as ratios relative to the control MSC group.

Xenograft *in vivo* Angiogenesis Assay
For the *in vivo* angiogenesis study, MSCs mixed with Matrigel were used (Melero-Martin and Bischoff, 2008). Briefly, MSCs were cultured in T175 flasks with DMEM/F-12 supplemented with 10% FBS. After 3 days of VitD3 treatment, 1×10^7 cells in each group were mixed with ice-cold Matrigel and subcutaneously injected into both flanks (two injections per mouse) of 8-week old C57BL/6 male mice. Three mice in each group received a total of six injections. Three weeks later, mice were euthanized and explanted Matrigel plugs were evaluated for color change due to perfusion with blood. Matrigel plugs were sectioned and stained with fluorescein-conjugated

isolectin B4 followed by image acquisition using a Leica laser scanning confocal microscope (Leica TCS SPE) (Chen et al., 2017). Capillaries were counted on images from 4 plugs in each group and expressed per mm2.

Gene Expression Analysis by Quantitative Real-time PCR
Total RNA was isolated from MSCs with TRIzol reagent (Invitrogen, 15596018) and 1 µg of RNA from each sample was reverse transcribed into cDNA by the First-strand cDNA synthesis system (Bio-Rad, 170-8841). The expression of genes related to angiogenesis and neovascularization was examined by qRT-PCR using Bullseye EvaGreen qPCR Master Mix (Midsci, BEQPCR-LR), cDNA template, and forward and reverse primers (**Table S1**) using ViiA™ 7 Real-Time PCR System (Applied Biosystems). GAPDH was used as endogenous control and $2^{-\Delta\Delta CT}$ method was used for data analysis (Zhao et al., 2019).

Western Immunoblotting
Cell extracts were lysed in radio-immunoprecipitation assay buffer (RIPA) supplemented with protease inhibitors (Roche Diagnostics, 04693124001). Protein concentration was determined by Pierce BCA Protein Assay kit (Fisher, 23224). SDS-Polyacrylamide Gel Electrophoresis (SDS-PAGE) was performed following standard methods (Zhao et al., 2019). Following transfer, the membrane was probed with primary antibodies and labelled using fluorescently conjugated secondary antibodies (LI-COR Biosciences, 925-68072 and 925-32213) visualized using an Odyssey scanner (LI-COR Biosciences). Densitometry analysis was performed using the Image Studio software supplied by LI-COR Bioscience. The densitometric values of all bands of interest were normalized to β-actin (loading control).

Immunofluorescence Assay
MSCs were plated on glass bottom plates. Following VitD3 treatment, MSCs were rinsed with PBS, fixed with 4% paraformaldehyde, permeabilized with 0.3% Triton X-100 (BD Cytofix/Cytoperm fixation/permeabilization kit; BD biosciences, 554714), blocked with 10% donkey serum for 1 h, and incubated with primary antibodies overnight at 4°C followed by secondary antibodies (Invitrogen, A16004 and A18740). Image acquisition was performed using an Olympus IX71 fluorescent microscope.

Flow Cytometry
VitD3-treated MSCs were immunostained in FACS buffer (0.1% BSA in PBS) with PE-conjugated anti-CD34 and FITC-conjugated anti-CD31 antibodies. Flow cytometric analysis of endothelial cell surface markers was performed using a BD™ LSR II and FlowJo software following established methods (Adamiak et al., 2018).

Chromatin Immunoprecipitation
To identify potential VDR protein response elements, we searched the IGF-1 promoter region for the VDR binding motif (Ramagopalan et al., 2010). For the chromatin immunoprecipitation assay, MSCs were subjected to VitD3 treatment, and then cross-linked with 1% formaldehyde for 15 mins at room temperature. The crosslinking was stopped by the addition of 125 nM glycine (final concentration). Cell lysates were sonicated to generate DNA fragments with an average size of less than 1,000 bp and immunoprecipitated with VDR-specific antibody. Bound DNA fragments were eluted and amplified by PCR with specific primers (**Table S1**).

Plasmid Construction and Luciferase Reporter Assay
For the reporter assay, the IGF-1 genomic fragments (-2111 to +11) containing either wild-type or mutant VDR binding regions (**Figure 6A**) were amplified from murine genomic DNA using Phusion High-Fidelity DNA Polymerase (NEB, M0530) and subcloned into pGL3-basic vector

(Promega, catalog # E1751). The site-directed mutagenesis of the VDR binding region was performed following the In-Fusion® HD Cloning Plus Kit (Takara, Japan) with IGF-1 mutation primers (**Table S1**). The DNA fragment of the IGF-1 promoter was subcloned into the firefly-luciferase reporter vector, pGL3-Basic (renamed pGL3-IGF-1-wt). The VDR binding elements within the IGF-1 promoter region were mutated and subcloned into the pGL3-Basic vector and renamed pGL3-IGF-1-mut1 and pGL3-IGF-1-mut2 (**Figure 6A**).

The luciferase reporter assay was performed following the manufacturer's protocol. Briefly, MSCs were transfected with reporter vectors (pGL3-IGF-1-wt, pGL3-IGF-1-mut1 and pGL3-IGF-1-mut2) by Lipofectamine™ 3000 (Invitrogen, L3000001). After 48 h of VitD3 treatment, luciferase activity was determined using a Dual Luciferase Assay System (Promega, E2920). Transfection efficiency was normalized on the basis of Renilla luciferase activity co-transfected with pRL-TK vector (Promega, E2241).

IGF-1 ELISA assay
IGF-1 concentration in culture media was quantified using Invitrogen Mouse IGF-1 ELISA Kit (EMIGF1) following the manufacturer's instructions.

Cytodex Beads Branching Assay
The C57BL/6 Mouse Pulmonary Artery Endothelial Cells (MAECs) from Creative Bioarray (CSC-C4244X) are isolated from pulmonary artery of pathogen-free mice and maintained using EBM-2MV complete media. The Cytodex bead branching assay was performed as previously described (Nakatsu et al., 2003). Briefly, MAECs were incubated in suspension with Cytodex beads at a ratio of $1x10^6$ cells per 1,200 beads for 4 h at 37°C with occasional agitation. After dilution in the pre-gel solution at a concentration of 500 beads per mL, MAEC beads were maintained on Fibrinogen (Type I) pre-coated 12-well plates and co-cultured with VitD3-treated MSCs in EGM-2MV media. To block IGF-1 activity, 1 µM of PPP was added to the VitD3-MSCs and MAEC beads co-culture system. Medium was changed every other day. Phase contrast images of branching tubes were acquired. The length of 8 randomly selected protrusions from each of 10 independent beads in each group was measured using the ImagePro Plus software and the average lengths calculated. The number of protrusions on each of these independent beads were also counted on digital images.

Aortic Ring Assay for *Ex Vivo* Angiogenesis
Aortic ring assay was performed according to published methods (Bellacen and Lewis, 2009). Thoracic aortic segments were harvested from 8-week-old male C57BL/6 mice under a dissecting microscope, cut into 1 mm sections, and embedded in Matrigel-coated plates. Aortic sections were then co-cultured with VitD3-treated MSCs and maintained in EBM-2MV endothelial culture medium. To examine the role of IGF-1, PPP was added to block IGF-1 activity in the co-culture system. Five microscopic images were acquired from each group. Using ImagePro Plus software, the areas were drawn manually. The total aortic spouting area (surface area of the aortic ring plus the sprouting area) as well as the area of the aortic ring alone were measured in each digital image. Data were expressed as the ratio of the total aortic sprouting area and the aortic ring surface area alone.

Statistical Analysis
Data are expressed as means ± SEM. Statistical comparisons were performed using the SPSS software version 26.0 (IBM, Armonk, NY). One-way or Welch's ANOVA with Bonferroni or Dunnett's T3 *post hoc* tests, respectively, were performed to assess significance. Significance for all statistical tests was shown in figures for not significant (NS), $p < 0.05$ (*), $p < 0.01$ (**), $p < 0.001$ (***) and $p < 0.0001$ (****).

REFERENCES

Adamiak, M., Cheng, G., Bobis-Wozowicz, S., Zhao, L., Kedracka-Krok, S., Samanta, A., Karnas, E., Xuan, Y.T., Skupien-Rabian, B., Chen, X.*, et al.* (2018). Induced Pluripotent Stem Cell (iPSC)-Derived Extracellular Vesicles Are Safer and More Effective for Cardiac Repair Than iPSCs. Circ Res *122*, 296-309.

Bellacen, K., and Lewis, E.C. (2009). Aortic ring assay. Journal of visualized experiments : JoVE.

Chen, L., Zhao, L., Samanta, A., Mahmoudi, S.M., Buehler, T., Cantilena, A., Vincent, R.J., Girgis, M., Breeden, J., Asante, S.*, et al.* (2017). STAT3 balances myocyte hypertrophy vis-a-vis autophagy in response to Angiotensin II by modulating the AMPKalpha/mTOR axis. PloS one *12*, e0179835.

Khoo, C.P., Micklem, K., and Watt, S.M. (2011). A comparison of methods for quantifying angiogenesis in the Matrigel assay in vitro. Tissue engineering. Part C, Methods *17*, 895-906.

Labedz-Maslowska, A., Lipert, B., Berdecka, D., Kedracka-Krok, S., Jankowska, U., Kamycka, E., Sekula, M., Madeja, Z., Dawn, B., Jura, J.*, et al.* (2015). Monocyte Chemoattractant Protein-Induced Protein 1 (MCPIP1) Enhances Angiogenic and Cardiomyogenic Potential of Murine Bone Marrow-Derived Mesenchymal Stem Cells. PloS one *10*, e0133746.

Melero-Martin, J.M., and Bischoff, J. (2008). Chapter 13. An in vivo experimental model for postnatal vasculogenesis. Methods in enzymology *445*, 303-329.

Nakatsu, M.N., Sainson, R.C., Aoto, J.N., Taylor, K.L., Aitkenhead, M., Perez-del-Pulgar, S., Carpenter, P.M., and Hughes, C.C. (2003). Angiogenic sprouting and capillary lumen formation modeled by human umbilical vein endothelial cells (HUVEC) in fibrin gels: the role of fibroblasts and Angiopoietin-1. Microvascular research *66*, 102-112.

Ramagopalan, S.V., Heger, A., Berlanga, A.J., Maugeri, N.J., Lincoln, M.R., Burrell, A., Handunnetthi, L., Handel, A.E., Disanto, G., Orton, S.M.*, et al.* (2010). A ChIP-seq defined genome-wide map of vitamin D receptor binding: associations with disease and evolution. Genome research *20*, 1352-1360.

Zhao, L., Cheng, G., Choksi, K., Samanta, A., Girgis, M., Soder, R., Vincent, R.J., Wulser, M., De Ruyter, M., McEnulty, P.*, et al.* (2019). Transplantation of Human Umbilical Cord Blood-Derived Cellular Fraction Improves Left Ventricular Function and Remodeling After Myocardial Ischemia/Reperfusion. Circ Res *125*, 759-772.

TRANSPARENT METHODS

Key Resources

REAGENT or RESOURCE	SOURCE	IDENTIFIER
Antibodies		
anti-CD34	Novus Biologicals	NB600-1071
anti-VE-cadherin	Novus Biologicals	AF1002
anti-VEGF	Santa Cruz Biotechnology	sc-152
anti-FLK1	Santa Cruz Biotechnology	sc-57135
anti-VDR	Cell Signaling Technology	#12550
anti-IGF-1	Santa Cruz Biotechnology	sc-1422
anti-IGF-1R	Cell Signaling Technology	#9750
anti-pIGF-1R	Cell Signaling Technology	#3021
anti-pERK1/2	Cell Signaling Technology	#4370
anti-β-Actin	Santa Cruz Biotechnology	sc-1616
PE-labeled anti-CD34	BD Biosciences	#551387
FITC-labeled anti-CD31	eBioscience	E00252-1631
Donkey anti-Goat IgG (H+L), TRITC	Invitrogen	A16004
Donkey anti-Rat IgG (H+L), FITC	Invitrogen	A18740
IRDye® 800CW Donkey anti-Rabbit IgG	LI-COR Biosciences	925-32213
IRDye® 680RD Donkey anti-Mouse IgG	LI-COR Biosciences	925-68072
GSL I - Isolectin B4	Vector Laboratories Ltd	FL1201
Chemicals, Peptides, and Recombinant Proteins		
DMEM/F-12	Corning	10-090-CV
FBS	Gibco	26140-079
Ficoll	GE healthcare	17-1440-02
DMEM	Gibco	11330-032
1α,25-Dihydroxyvitamin D3	Sigma-Aldrich	D1530-10UG
Cytodex 3 microcarrier beads	Sigma-Aldrich	C3275-10G
Fibrinogen	Sigma-Aldrich	F6755
Picropodophyllin	Sigma-Aldrich	407247
Phusion High-Fidelity DNA Polymerase	NEB	M0530
Matrigel matrix	BD Biosciences	354267
ImagePro Plus software	Media Cybernetics	http://www.mediacy.com/imagepro
TRIzol reagent	Invitrogen	15596018
EverGreen qPCR master mix (2x)	MIDSCI	BEQPCR-LR
BSA	Fisher Scientific	BP9706100
Donkey serum	Fisher Scientific	56-646-05ML
RIPA buffer	Fisher Scientific	AAJ63306AK
Protease inhibitors	Roche Diagnostics	04693124001
Triton X-100	Fisher Scientific	BP151-100
CellTrace™ Calcein Green, AM	Fisher Scientific	C34852

Lipofectamine™ 3000	Invitrogen	L3000001

Critical Commercial Assays

Cytofix/Cytoperm fixation/permeabilization kit	BD Bisosciences	554714
In-Fusion® HD Cloning Plus Kit	Takara	638909
BCA protein assay kit	Fisher Scientific	23224
Lonza Walkersville EGM 2 BULLET KIT	Lonza	cc-3162
Fist strand cDNA synthesis system	Bio-Rad	170-8841
Dual-Glo™ Luciferase Assay System	Promega	PR-E2920
IGF-1 Mouse ELISA Kit	Invitrogen	EMIGF1

Recombinant DNA

pGL3-basic vctor	Promega	E1751
pRL-TK vector	Promega	E2241

Experimental Models: Organisms/Cell

C57BL/6 mouse	The Jackson Laboratory	
MAEC	Creative Bioarray	CSC-C4244X

TRANSPARENT METHODS

Table S1. Primers used in the study, related to Figures 1, 4, 6.

PRIMERS FOR QPCR		
NAME	**SEQUENCE 5'-3'**	**GENE ID**
GAPDH-F	AGGTCGGTGTGAACGGATTTG	NM_008084
GAPDH-R	TGTAGACCATGTAGTTGAGGTCA	
c-Myc-F	GCCCCTAGTGCTGCATGAG	NM_010849.4
c-Myc-R	CCACAGACACCACATCAATTTCTT	
Oct4-F	GGAGTCTGGAGACCATGTTTCTG	NM_013633.2
Oct4-R	GAACCATACTCGAACCACATCCTT	
SSEA1-F	ACGGATAAGGCGCTGGTACTA	NM_010242
SSEA1-R	GGAAGCCATAGGGCACGAA	
VEGF-F	CTGCCGTCCGATTGAGACC	MMU50279
VEGF-R	CCCCTCCTTGTACCACTGTC	
Endothelin-1-F	GCACCGGAGCTGAGAATGG	NM_010104
Endothelin-1-R	GTGGCAGAAGTAGACACACTC	
VCAM-1-F	AGTTGGGGATTCGGTTGTTCT	NM_011693
VCAM-1-R	CCCCTCATTCCTTACCACCC	
ICAM-1-F	GTGATGCTCAGGTATCCATCCA	NM_010494
ICAM-1-R	CACAGTTCTCAAAGCACAGCG	
VWF-F	CTTCTGTACGCCTCAGCTATG	NM_011708
VWF-R	GCCGTTGTAATTCCCACACAAG	
FLK1-F	TTTGGCAAATACAACCCTTCAGA	NM_010612
FLK1-R	GCAGAAGATACTGTCACCACC	
PDGFrb-F	TTCCAGGAGTGATACCAGCTT	NM_001146268
PDGFrb-R	AGGGGGCGTGATGACTAGG	
αSMA-F	GTCCCAGACATCAGGGAGTAA	NM_007392
αSMA-R	TCGGATACTTCAGCGTCAGGA	
IGF1-F	CTGGACCAGAGACCCTTTGC	NM_001111274
IGF1-R	GGACGGGGACTTCTGAGTCTT	
CD34-F	AAGGCTGGGTGAAGACCCTTA	NM_001111059
CD34-R	TGAATGGCCGTTTCTGGAAGT	
VE-cadherin-F	CACTGCTTTGGGAGCCTTC	NM_009868
VE-cadherin-R	GGGGCAGCGATTCATTTTTCT	
PRIMERS FOR RECONSTRUCTION		
IGF1-F-XhoI	GCACTCGAGTCTCACACCAGGTTTCTAA	NM_010512
IGF1-R-HindIII	CGGTACCAAGCTTACAGGAAACAGCT	
Mut-F1	TCCTTCGCCAGTAGGTAGTGACAGGCATC	
Mut-R1	GATGCCTGTCACTACCTACTGGCGAAGGA	
Mut-F2	TACCCTCACTATGTCACAATTAACAGCATTG	
Mut-R2	CAATGCTGTTAATTGTGACATAGTGAGGGTA	
PRIMERS FOR ChIP ASSAY		
ChIP-IGF1-F1	CATCATAACCCTGGAGAGAGTATTG	NM_010512
ChIP-IGF1-R1	GCTGAGATCTGGGATGGATTG	